Processing measured geomembrane deformations to strains with FEA

R.J. Minnaar
Advanced Structural Mechanics (Pty) Ltd, Pretoria, South Africa

S. Chaperon & I. de Villiers
TANDM Technologies (Pty) Ltd, Pretoria, South Africa

ABSTRACT: Tailings storage facilities and landfill sites are often lined with a HDPE geomembrane to protect the underlying environment from contamination by leachate. To achieve the desired performance over the lifetime of the facility, limits are placed on the peak tensile strain to which the geomembrane may be subjected under operational conditions. Experimental methods have been developed to record the operational deformations onto metal foil sheets. The actual experimental methods are not considered in this study. Once the deformed sheets have been recovered, 3D scanning techniques are typically used to quantify the deformations and to map them onto a millimetre square grid. In South Africa, two approximations are widely used to estimate the geomembrane strains from the measured deformation. This study reviews the implications of the assumptions included in these approximations. Furthermore, the approximation results are compared to a more rigorous treatment of the same measured deformations using finite element analysis. The finite element analysis is not used to analyse the deformation of the geomembrane or the foil sheet, but only to calculate the strains from the measured deformation distribution. The advantage of this approach is that it accounts for the in-plane response of the geomembrane. As a result, the derived strains are more realistic. The magnitudes of possible errors in the approximated strains are quantified for various deformation characteristics.

1 INTRODUCTION

New landfill sites and tailings storage facilities are lined with containment barrier systems that separate the stored material and its leachate from the environment and groundwater below. These barrier systems comprise various layers, which often include a continuous high-density polyethylene (HDPE) geomembrane of 1.5 mm to 2 mm thickness. A typical containment barrier system is shown in Figure 1.

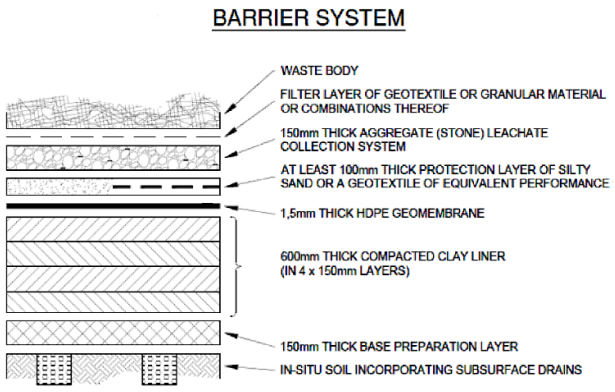

Figure 1. Typical containment barrier system including HDPE geomembrane

Eldesouky & Brachman (2018) state that the tensile strains in HDPE geomembranes need to be limited to prevent brittle rupture and an increase in leakage over time. The current study is not concerned with the actual limiting tensile strain values, only with the accurate determination of the maximum tensile strain from measurement data.

Various approaches have been proposed to record the geomembrane liner deformation onto metal foil sheets (Hornsey & Wishaw 2012, Chaperon et al. 2021). In these approaches, a metal foil sheet is placed directly under the geomebrane in the barrier system, as shown in Figure 2.

Figure 2. Metal foil sheet placed on compacted clay layer with geomembrane temporarily folded away

The test section is then loaded to the full operational load of the barrier system. The membrane deformation is recorded through plastic yielding of the foil sheet. The experiment may be performed in the laboratory or in the field. The foil sheets are carefully recovered after the application of the load and the deformation of the foil is measured with 3D scanning technology and mapped onto a 1 mm × 1 mm grid

In South Africa, the methodologies proposed by Hornsey & Wishaw (2012) and Tognon et al. (2000) are generally used to estimate the maximum tensile geomembrane strains from the scanned deformation data. This paper proposes an alternative methodology based on finite element analysis (FEA) and compares the results to the generally used methodologies.

2 STRAIN IN HDPE GEOMEMBRANES

A discussion of the strain in geomembranes is preceded by a discussion of the strain in a 1-dimensional beam.

2.1 *Contributions to the total tensile strain in a beam*

The total tensile strain in the outer fibres of a beam is made up of the *bending* and the *membrane* strain components i.e.:

$$\epsilon_{total} = \epsilon_{bend} + \epsilon_{memb} \quad (1)$$

The reference to membrane strain is taken from plate and shell nomenclature and does not refer to the geomembrane. The bending strain (ϵ_{bend}) is, as the name indicates, a result of pure bending, and is generally assumed to vary linearly across the thickness of the beam. The membrane strain (ϵ_{memb}), on the other hand, is a result of an axially applied tensile or compressive load on the beam. The membrane strain is constant across the thickness of the beam. Depending on the sign of the axial load, the membrane strain increases or decreases the total tensile strain in the outer fibres. The contribution of the bending and membrane components to the total strain in the beam is illustrated in Figure 3.

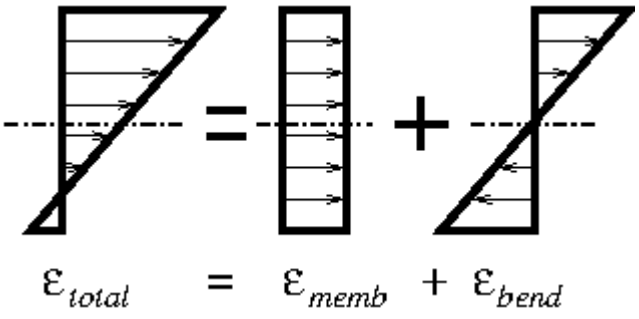

Figure 3. Summation of membrane and bending strain to arrive at total strain

2.2 *Extension to two-dimensional plates and shells*

The above arguments of bending and membrane contributions to the total strain also hold for plates and shells. However, these strains are now two-dimensional fields. Since it is the maximum tensile strain which is relevant to the assessment of HDPE geomembranes, the maximum principal strain is a convenient measure which accounts for the two-dimensional strain field.

3 REVIEW OF THE STRAIN APPROXIMATIONS WIDELY USED IN SOUTH AFRICA

The strain approximations proposed by Hornsey & Wishaw (2012) and Tognon et al. (2000) are widely used in South Africa to estimate geomembrane strains from deformed metal foil sheets. In both approaches, the plates are 3D scanned and the measured vertical offset from a theoretical neutral flat plane is discretized onto a 1 mm × 1 mm square grid. The differences between the approaches are discussed below.

3.1 *Approximation of Hornsey & Wishaw (2012)*

This approach uses the theorem of Pythagoras to estimate the membrane strain between adjacent points. With the nomenclature of Figure 4, it is expressed as:

$$\epsilon_{memb} = \frac{\sqrt{(w_i - w_{i-1})^2 + (x_i - x_{i-1})^2}}{(x_i - x_{i-1})} - 1 \quad (2)$$

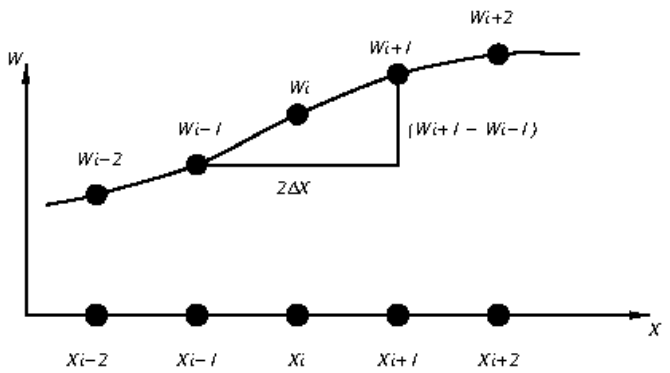

Figure 4. Data points used for membrane strain approximation

The implicit assumption in this membrane strain approximation is that all points only move vertically. The membrane strain estimate is therefore purely a function of the lengthening associated with the vertical offset and no allowance is made for any lateral movement of the points being monitored. Accordingly, the approximated membrane strain is directly related to the gradient of the deformation. This, in turn, implies that the maximum membrane strain will always occur at the point or area of maximum gradient.

This is counterintuitive when thinking about a membrane being forced over a protrusion or bulge. Intuitively, the peak membrane strain or stretch would be expected over the apex of the protrusion.

It should also be noted that no attempt is made to estimate bending strain. Any contribution of bending strains is therefore completely omitted from the Hornsey & Wishaw (2012) strain estimate.

3.2 *Approximation of Tognon et al. (2000)*

This approach separately estimates the membrane and bending strains. The membrane strain is obtained from a first-order central difference approximation (see Fig. 4 for nomenclature):

$$\epsilon_{memb} = \sqrt{1 + \left(\frac{\mathrm{d}w}{\mathrm{d}x}\right)^2} - 1 \tag{3}$$

$$\epsilon_{memb} = \sqrt{1 + \left(\frac{1}{2\Delta x}[w_{i+1} - w_{i-1}]\right)^2} - 1 \tag{4}$$

The above approach is very similar to the Hornsey & Wishaw (2012) approach, but considers three, rather than two points. However, the assumption of no lateral movement remains.

The bending strain is obtained from a second-order central difference approximation:

$$\epsilon_{bend} = -z\frac{\mathrm{d}^2 w}{\mathrm{d}x^2} \tag{5}$$

$$\epsilon_{bend} = \frac{-z}{\Delta x^2}[w_{i+1} - 2w_i + w_{i-1}] \tag{6}$$

where z is the distance from the neutral axis to the outer fibre of the geomembrane.

The bending approximation follows the established theory that the bending strain is related to curvature. The curvature is captured accurately by the deformed foil and is not influenced by assumptions regarding the lateral movement of the measuring points. The bending strains estimated in this manner may therefore be expected to be accurate, since the only approximation is in the manner in which the discretized points represent the actual curvature.

Despite the accurate bending strain approximation, the complete Tognon et al. (2000) approximation still includes the issues with the membrane strain approximation, discussed above, namely that all points only move vertically and accordingly, that membrane strain is directly related to the gradient of the deformation.

4 DATA PROCESSING WITH FINITE ELEMENT ANALYSIS

As an alternative to the above approximations, it is proposed that the measured deformations be processed with a finite element analysis (FEA). To this end, the measured vertical displacements are considered as prescribed displacements of a finite element mesh that corresponds exactly to the grid to which the scanned data has been discretized.

The analysis does therefore not solve for any vertical displacements, but rather only solves for the total geomembrane strains associated with the measured vertical displacements.

4.1 *Modelling lateral displacements*

When the geomembrane deforms, there is no mechanism forcing points to only move along vertical lines, as is assumed in the discussed membrane strain approximations. In the FE analysis, the nodes are free to move laterally and the membrane strain distribution in the geomembrane is governed by the stiffness of the HDPE material.

However, by restraining the lateral degrees of freedom of all the prescribed nodes, the FE analysis can represent the boundary conditions assumed in the membrane strain approximations. This allows for a direct comparison of the approximations and the FE results (see Sections 5 & 6 below).

4.2 *Inclusion of material and geometric non-linearities*

Performing an FE analysis to process the measured geomembrane deformations allows for material and geometric non-linearities to be included.

Material non-linearity stems from the fact that HDPE does not exhibit a linear stress-strain relationship over the strain range of interest. The considered stress-strain curve is taken from Patlazhan et al. (2008) and is shown in Figure 5. Only the loading portion of the curve is of interest here, since the HDPE is not unloaded in the geomembrane application.

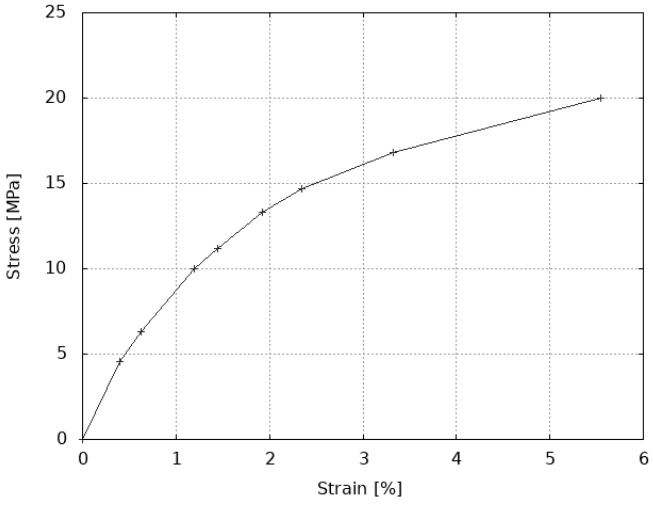

Figure 5. Stress-strain curve for HDPE (Patlazhan et al. 2008)

Geometric non-linearity is included in the analyses to ensure that the lateral movement of measuring

points is taken into account (linear analyses only consider the initial geometry and will therefore ignore any lateral movement of the measuring points).

4.3 *Effect of foil sheet offset from membrane neutral axis*

The scanned metal foil profile represents the deformation of either the upper or lower surface of the geomembrane, depending on the location of the foil sheet during the test. Strictly speaking, a correction should be applied to derive the deformation profile of the geomembrane mid-surface. Neglecting any thinning of the geomembrane, this can be achieved through a simple numerical transformation.

In this investigation, no correction was applied, and the sheet profile was assumed to represent the mid-surface of the geomembrane. This simplification is deemed to be acceptable for the purposes of this study, considering the geomembrane thickness of 1.5 mm to 2.0 mm.

5 TEST PROBLEMS

Three test deformation geometries were considered to allow for simple comparisons between the methods. The geometries are all axisymmetric sine-shaped bumps of varying diameters. The amplitudes were chosen such that all three bumps have the same maximum curvature and therefore the same maximum bending strains. The parameters of the considered bumps are listed in Table 1 and the bumps and their derivatives are shown in Figures 6 and 7.

Table 1. Parameters of axisymmetric sine-shaped bumps

	Radius [mm]	Amplitude [mm]	Peak-to-peak [mm]
Bump #1:	50	5.00	10.0
Bump #2:	25	1.25	2.5
Bump #3:	10	0.20	0.4

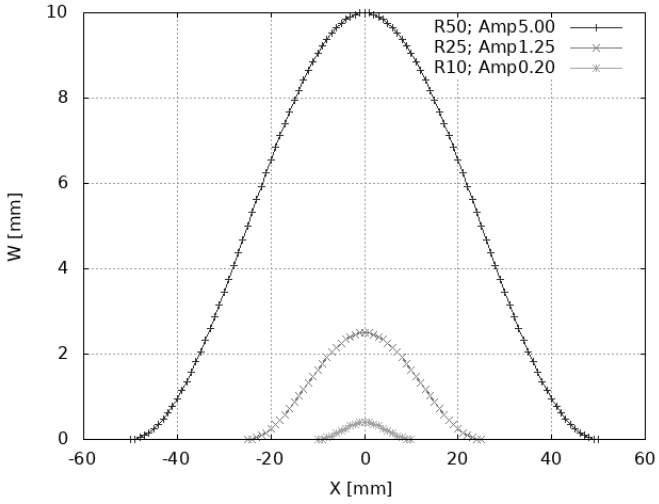

Figure 6. Profiles of considered sine-shaped bumps

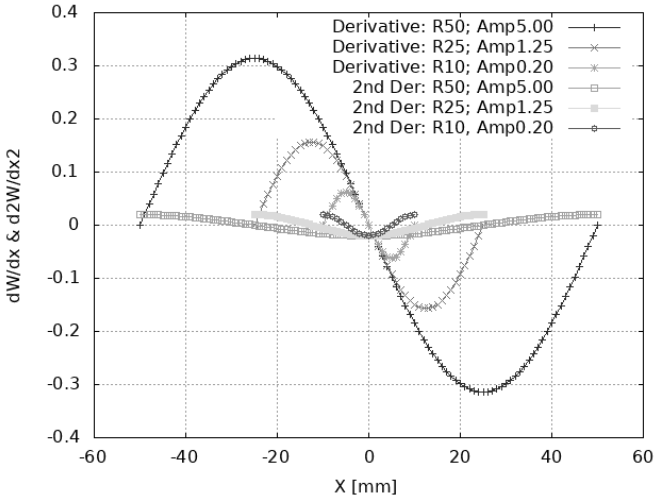

Figure 7. First and second derivatives of considered sine-shaped bumps

Analyses were performed for all three bumps for the cases where the lateral displacements are fixed (approximations) and free (realistic). Plots of the membrane, bending and total strains are provided in Figures 8-10, and the results are summarized in Table 2.

Table 2. Comparisons of FEA and approximated tensile strains for sine-shaped bumps

	FEA	Approximation (laterally fixed)	Approximation as % of FEA
Membrane strain			
Bump #1 (Fig. 8):	2.2%	4.9%	219%
Bump #2:	0.6%	1.2%	198%
Bump #3:	0.1%	0.2%	236%
Bending strain			
Bump #1 (Fig. 9):	1.9%	2.0%	102%
Bump #2:	1.9%	1.9%	101%
Bump #3:	1.8%	1.8%	100%
Total strain (membrane + bending)			
Bump #1 (Fig. 10):	4.1%	5.1%	122%
Bump #2:	2.5%	2.0%	79%
Bump #3:	1.9%	1.8%	96%

From the plots and the summarized results, the following should be noted:

- For the membrane strains, the approximations overestimate the peak strain, but the distribution is incorrect, with the approximated peak occurring at the maximum gradient, rather than at the apex (see Fig. 8). This is as a result of the assumption that there is no lateral displacement, while the actual geomembrane stretches over the entire bump, thus distributing the membrane strain.
- The approximation of the bending strain is very good. This is to be expected since the curvature, which governs the bending strain, is accurately captured by the approximation, despite the assumption of no lateral movement (see Fig. 9).

- The total strain is influenced by the incorrect distribution of the membrane strain approximation (see Fig. 10). This is clearly illustrated in the case of Bump #2. While the membrane strain approximation is at 198% of the FEA value, the total strain approximation is at only 79% of the FEA value i.e. an underestimation of the maximum strain.
- Finally, when assessing the approximation of Hornsey & Wishaw (2012) (membrane strain only) the comparison should be to the total FEA strain and not the membrane FEA strain, since the acceptance criteria is based on total tensile strain. The estimates then drop to 48% and 10%, for Bumps #2 and #3, respectively.

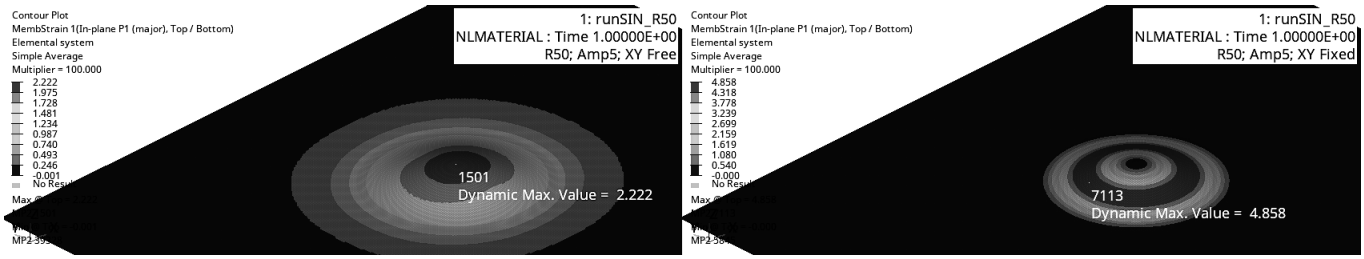

Figure 8. Membrane strain distribution of 100 mm sine-shaped bump; LHS – Lateral free; RHS – Lateral restrained (approximation)

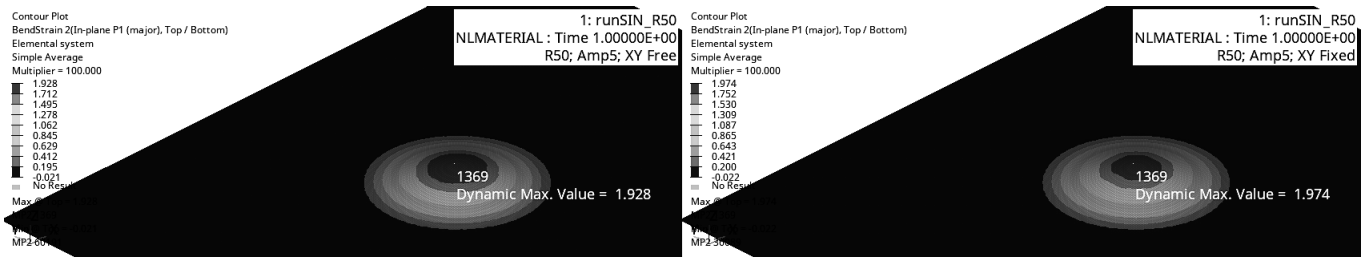

Figure 9. Bending strain distribution of 100 mm sine-shaped bump: LHS – Lateral free; RHS – Lateral restrained (approximation)

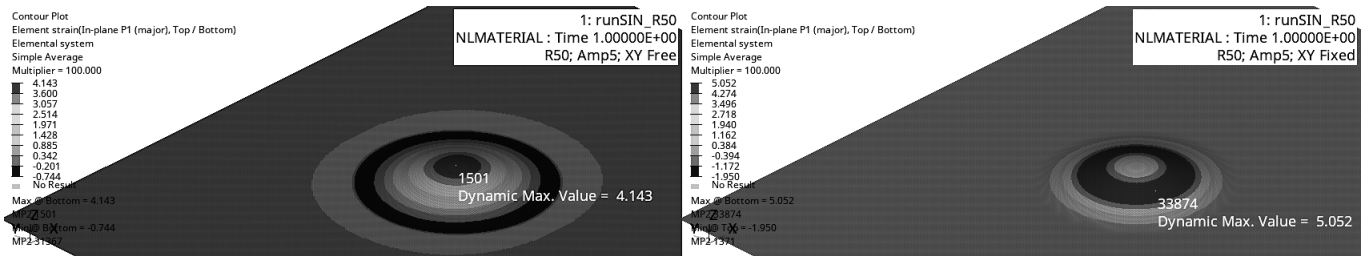

Figure 10. Total strain distribution for 100 mm sine-shaped bump: LHS – Lateral free; RHS – Lateral restrained (approximation)

6 ACTUAL MEASURED TEST DATA

A similar comparison is performed for three sets of actual measured test data. In these cases, the comparison is always to the total strain, as calculated with the non-linear FEA. A typical result set is shown in Figure 11 with the measured deformation shown in Figure 12 (with a deformation scale factor of 20). The results for all three sets are summarized in Table 3. For completeness, the results for the three sine-shaped bumps are also included in the table.

From these results, it is clear that the method of Hornsey & Wishaw (2012) is not reliable and is likely to underestimate the maximum tensile strain, possibly by a significant margin. This is primarily due to the complete omission of the bending strain contribution.

The method of Tognon et al. (2000) is far more reliable, but there is still a chance of significantly underestimating the maximum strain, as seen for the case of Bump #2.

Table 3. Comparison of approximations to FEA results for actual measured data and sine-shaped bumps

	FEA ϵ_{total}	Hornsey & Wishaw (2012) ϵ_{memb}	Tognon et al. (2000) ϵ_{total}
Plate #1:	4.3%	3.0% (70%)	4.6% (108%)
Plate #2:	7.4%	3.8% (51%)	7.5% (101%)
Plate #3:	12.3%	8.2% (67%)	13.9% (113%)
Bump #1:	4.1%	4.9% (117%)	5.1% (122%)
Bump #2:	2.5%	1.2% (48%)	2.0% (79%)
Bump #3:	1.9%	0.2% (10%)	1.8% (96%)

The reliability of the Tognon et al (2000) method is subject to the nature of the particular protrusion or indentation. In the case that the membrane strain provides a significant contribution to the total strain, the unreliability in the magnitude and the distribution of the estimated membrane strains compromises the Tognon et al. (2000) estimate.

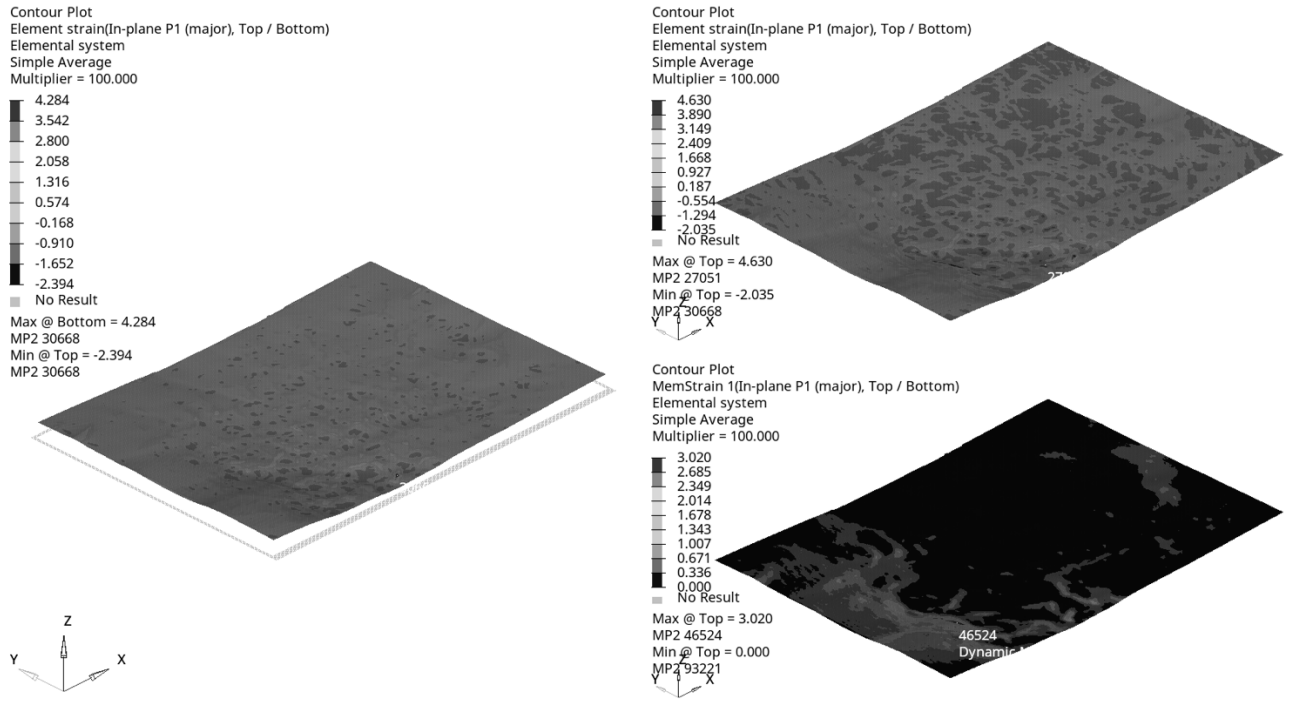

Figure 11. Actual data Plate #2: LHS – Lateral free; RHS Top – Lateral restrained membrane + bending (Tognon et al. (2000) approximation); RHS Bottom – Lateral restrained membrane only (Hornsey & Wishaw (2012) approximation).

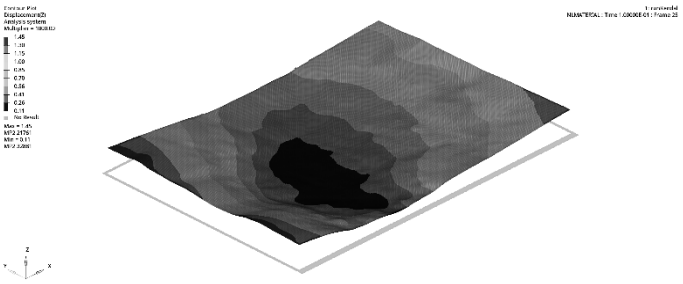

Figure 12. Actual data Plate #2: Measured deformation (vertical deflection) [mm] plotted with a deformation scale factor of 20

7 CONCLUSIONS

This study considered the data processing which is required to derive the maximum tensile strains in HDPE geomembranes from measured deformation profiles.

The approximations of Hornsey & Wishaw (2012) and Tognon et al. (2000), are widely used in South Africa. The results of these approximations were compared to a proposed method that uses non-linear FEA to process the measured data.

From the comparison of the results, it is concluded that the method of Hornsey & Wishaw (2012) is unreliable and is likely to underestimate the maximum tensile liner strains by a significant margin. While the method of Tognon et al. (2000) is more reliable, in one instance out of six, the maximum tensile strain was underestimated by a significant margin. The weakness in the Tognon et al. (2000) method stems from the membrane strain approximation which provides an inaccurate estimate of the membrane strain distribution.

The non-linear FEA which is used to process the measured deformation data is trivial when using modern commercial FE software, since the prescribed vertical displacements ensure quick convergence. The FEA approach is therefore deemed to be a feasible alternative to the currently used approximations. The FEA approach is both simple to apply and eliminates the uncertainties associated with the approximations.

REFERENCES

Chaperon, S., Legg, P. & Barnard, E. 2021. In-field geomembrane tensile strain determination for barrier system performance assessment. *Landfill and waste treatment virtual seminar and expo 3-5 November 2021:* Kwazulu-Natal landfill and waste treatment interest group.

Eldesouky, H.M.G. & Brachman, R.W.I. 2018. Calculating local geomembrane strains from a single gravel particle with thin-plate theory. *Geotextiles and Geomembranes* 46: 101-110.

Hornsey, W.P. & Wishaw, D.M. 2012. Development of a methodology for the evaluation of geomembrane strain and relative performance of cushion geotextiles. *Geotextiles and Geomembranes* 35: 87-99.

Patlazhan, S.A., Hizoum, K. & Rémond, Y. 2008. Stress-strain behaviour of high-density polyethylene below the yield point: Effect of unloading rate. *Polymer Science* (A) 50(5): 507-513.

Tognon, A.R., Rowe, R.K. & Moore, I.D. 2000. Geomembrane strain observed in large-scale testing of protection layers. *Journal of Geotechnical and Geoenvironmental Engineering* 126(12): 1194-1208.